RESEARCH PAPER

Factorial Optimization and Release Characterization of Microwave-Assisted Montelukast Sodium-Loaded Chitosan Nanobiocomposites

Mr. Ravikumar Bhikaji Misal[1*], Dr. Pravin S. Kawtikwar[2]
[1]Research Scholar, Department of Pharmaceutics,*
Sudhakarrao Naik Institute of Pharmacy, Pusad, Dist. Yavatmal.
Email: misalravi980@gmail.com.
[2]Principal, Department of Pharmaceutics,
Sudhakarrao Naik Institute of Pharmacy, Pusad, Dist. Yavatmal.
Email: pskawtikwar@rediffmail.com.

ABSTRACT
Montelukast sodium is clinically useful in asthma but its low aqueous solubility can constrain dissolution and formulation performance. This study developed a chitosan-based nanobiocomposite using ionic cross-linking with sodium tripolyphosphate followed by controlled microwave processing. A three-level, two-factor factorial design examined chitosan concentration and the chitosan-to-TPP mass ratio. Entrapment efficiency, particle size and zeta potential were treated as critical quality attributes. Nine batches were compared, and NB6 combined the highest observed entrapment efficiency (84.6 ± 1.7%) with the smallest mean particle size (172.6 ± 4.2 nm) and a positive zeta potential of 31.8 ± 1.1 mV. Drug release from the optimized material reached 91.2 ± 2.1% at 24 h and was described most closely by first-order and Higuchi models (R^2 0.968 and 0.960, respectively). The results show that polymer content and cross-linker ratio jointly govern nanoparticle compactness, drug retention and release. The work supports NB6 as a formulation-development lead, while scale-up, aerosol performance, stability and confirmatory pharmacokinetic testing remain necessary.

Keywords: montelukast sodium; chitosan; nanobiocomposite; microwave-assisted synthesis; factorial design; controlled release

How to cite this article: Ravikumar Bhikaji Misal1* Dr. Pravin S. Kawtikwar2. Factorial Optimization and Release Characterization of Microwave-Assisted Montelukast Sodium-Loaded Chitosan Nanobiocomposites. Int J Drug Deliv Technol. 2026;16(77s):1869-1876-1868. DOI: 10.25258/ijddt.16.77s.214.

1. Introduction

Asthma is sustained by airway inflammation, variable bronchoconstriction and heightened responsiveness to environmental or biological triggers. Montelukast sodium blocks cysteinyl leukotriene type 1 receptors and is used as maintenance therapy rather than as a rescue medicine. A formulation that disperses the drug efficiently and moderates its release may improve consistency of exposure without changing its pharmacological target.

Chitosan is a cationic, biodegradable polysaccharide whose amino groups become protonated in acidic media. Those groups permit ionic association with multivalent anions such as tripolyphosphate, allowing nanoparticles to form under comparatively mild conditions. The same surface charge can promote interaction with negatively charged mucosal components, although charge, size and polymer concentration must be balanced to avoid aggregation or excessive viscosity (Illum, 1998; Bhumkar & Pokharkar, 2006).

Microwave energy can shorten processing by producing rapid, volumetric heating. In a nanoparticle workflow, however, power and exposure must be controlled because local overheating can alter polymer chains or drug integrity. The present investigation therefore coupled ionic gelation with a bounded microwave step and used a factorial design to interpret formulation effects instead of selecting a batch from one-factor-at-a-time trials.

Quality-by-design thinking begins with a target product profile and links material attributes and process parameters to measurable outputs. For the current platform, entrapment efficiency indicates how successfully drug is retained, hydrodynamic diameter affects dispersion and biological interaction, and zeta potential provides an indirect measure of electrostatic stabilization. Release kinetics adds a functional test that connects structure with expected performance.

The objective was to prepare montelukast-loaded chitosan nanobiocomposites, quantify the influence of chitosan concentration and chitosan:TPP mass ratio, identify a balanced optimized batch, and characterize its release behavior. The dataset was taken from the attached thesis and is reported as a formulation-focused manuscript; animal efficacy outcomes are intentionally reserved for a separate article.

2. Materials and Methods

Montelukast sodium was obtained from Yarrow Pharmaceutical, Mumbai. Chitosan served as the polymer, sodium tripolyphosphate as ionic cross-linker, crosspovidone as stabilizing excipient, polyethylene glycol 400 as plasticizer and citric acid as a pH-adjusting component. Analytical-grade solvents and purified water were used throughout.

Identity testing included capillary melting point,

ultraviolet spectrophotometry, Fourier-transform infrared spectroscopy and differential scanning calorimetry. The absorption maximum was established by scanning a suitably diluted solution from 200 to 400 nm. Calibration standards were prepared in phosphate buffer and analyzed at 345 nm. Linearity was checked by ordinary least-squares regression of absorbance against concentration.

For FTIR assessment, drug, polymer and drug-polymer preparations were dispersed in dry potassium bromide and scanned between 4000 and 400 cm-1. Characteristic bands were compared for retention, displacement or emergence of signals. DSC samples were sealed in aluminium pans and heated under nitrogen at 10°C/min over a range sufficient to capture the drug transition and polymer-related thermal events.

Chitosan was dissolved in 1% v/v acetic acid under stirring. Montelukast sodium was dispersed into the polymer solution, after which 0.1% w/v TPP was added dropwise under continuous mixing to initiate ionic gelation. Crosspovidone and PEG 400 were incorporated before the dispersion underwent a controlled microwave exposure within the thesis-defined ranges of 100-800 W, 30-300 s and 40-80°C. Nanoparticles were isolated by refrigerated centrifugation, washed and redispersed. The selected batch was pre-frozen and lyophilized.

A 3^2 factorial design investigated chitosan concentration at 0.10, 0.25 and 0.40% w/v and chitosan:TPP mass ratio at 1.5, 2.5 and 3.5. Nine experimental batches were produced. Responses were entrapment efficiency, particle size and zeta potential. The preferred region combined high entrapment, smaller size and an absolute surface potential compatible with dispersion stability.

Entrapment was measured indirectly. Dispersions were centrifuged at 15,000 rpm for 30 min at 4°C, and free montelukast in the supernatant was quantified at 345 nm. Entrapment efficiency was calculated as the difference between added and free drug divided by the added drug, multiplied by 100. Measurements were performed in triplicate.

Dynamic light scattering at 25°C and a backscatter angle of 173° provided the intensity-weighted hydrodynamic diameter. Electrophoretic mobility was measured in a folded capillary cell and converted to zeta potential. Triplicate results are expressed as mean ± standard deviation. A polydispersity index at or below 0.30 was considered supportive of a relatively narrow distribution.

For release testing, the optimized formulation was placed in a dialysis membrane system against phosphate buffer maintained at physiological temperature. Samples were removed at predetermined intervals and replaced with fresh medium. Drug concentration was determined spectrophotometrically, cumulative release was corrected for sampling, and profiles were fitted to zero-order, first-order, Higuchi and Korsmeyer-Peppas equations (Fu & Kao, 2010).

Table 1. Factor levels used in the 3^2 design

Factor	Low (-1)	Middle (0)	High (+1)
Chitosan (% w/v)	0.10	0.25	0.40
Chitosan:TPP ratio	1.5	2.5	3.5
Interpretation: The three-level design spans the selected polymer concentration and chitosan:TPP ratio ranges, enabling evaluation of main and combined formulation effects.			

Table 2. Formulation responses (mean ± SD, n = 3)

Batch	Chitosan	Ratio	EE (%)	Size (nm)	ZP (mV)
NB1	0.25	2.5	68.4 ± 2.1	225.4 ± 5.6	+22.5 ± 1.2
NB2	0.40	1.5	72.1 ± 1.9	218.3 ± 4.8	+24.3 ± 1.5
NB3	0.25	3.5	75.8 ± 2.4	210.7 ± 6.2	+26.1 ± 1.3
NB4	0.10	2.5	70.2 ± 2.0	221.8 ± 5.1	+23.6 ± 1.0
NB5	0.40	3.5	80.5 ± 1.8	189.5 ± 4.5	+29.4 ± 1.2
NB6	0.25	2.5	84.6 ± 1.7	172.6 ± 4.2	+31.8 ± 1.1
NB7	0.10	1.5	69.6 ± 2.2	223.7 ± 5.4	+22.9 ± 1.3
NB8	0.10	3.5	77.3 ± 1.9	204.8 ± 4.9	+27.5 ± 1.2
NB9	0.40	2.5	82.2 ± 1.6	181.4 ± 4.1	+30.2 ± 1.0
Interpretation: NB6 provided the best balanced profile, with the highest entrapment efficiency, smallest particle size and strongest positive zeta potential among the tested batches.					

3. Results

Table 3. Cumulative release from NB6

Time (h)	Cumulative release (%)
0.5	12.5 ± 1.2
1	20.4 ± 1.5
2	32.1 ± 1.8
4	46.8 ± 2.0
6	58.9 ± 2.2
8	68.7 ± 2.3
12	79.4 ± 2.4
24	91.2 ± 2.1
Interpretation: NB6 showed a biphasic sustained-release pattern, progressing from	

12.5% at 0.5 h to 91.2% at 24 h.

Table 4. Release-model comparison

Model	Rate parameter	R^2
Zero order	k0 = 5.107	0.297
First order	k1 = 0.144	0.968
Higuchi	kH = 21.101	0.960
Korsmeyer-Peppas	n = 0.47	0.949
Interpretation: First-order kinetics gave the highest R-squared value, closely followed by the Higuchi model, indicating concentration-dependent release with a strong diffusion contribution.		

The observed melting point was 136°C, close to the reference value of 135.5°C. The UV method produced increasing absorbance over 5-35 µg/mL, supporting its use for routine quantification. FTIR retained the principal drug- and chitosan-associated bands without a new dominant signal, while thermal analysis supported physical incorporation rather than obvious chemical degradation.

Across the factorial batches, entrapment efficiency ranged from 68.4 ± 2.1% to 84.6 ± 1.7%. Mean particle size ranged from 172.6 ± 4.2 to 225.4 ± 5.6 nm, and zeta potential ranged from +22.5 ± 1.2 to +31.8 ± 1.1 mV. NB6 delivered the most favorable simultaneous response profile.

The optimized formulation showed an initial release of 12.5 ± 1.2% at 0.5 h, followed by a progressive increase to 91.2 ± 2.1% at 24 h. The early fraction can be attributed to drug located near the particle surface, whereas the slower phase is consistent with diffusion through, and relaxation of, the cross-linked polymeric matrix.

Model comparison favored first-order behavior (R^2 0.968) with a closely comparable Higuchi fit (R^2 0.960). Zero-order fit was weak (R^2 0.297). The Korsmeyer-Peppas exponent of 0.47 indicated predominantly diffusion-associated release with a possible contribution from polymer relaxation.

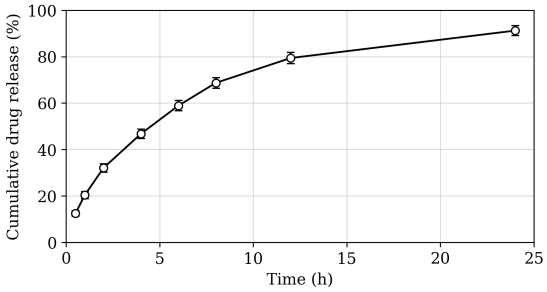

Figure 1. Cumulative montelukast sodium release from optimized batch NB6 (mean ± SD, n = 3).

3.1 Supplementary Calculated Results

Additional descriptive calculations were performed from the already reported batch means and release profile; no new laboratory observations were introduced. Relative to NB1, the optimized NB6 batch increased entrapment efficiency by 23.7%, reduced particle size by 23.4%, and increased the magnitude of the positive zeta potential by 41.3%. NB6 also exceeded the mean entrapment efficiency of all nine batches by 12.8% and remained 15.2% smaller than the overall mean particle size. These combined changes support its selection because improvement was achieved across all three critical quality attributes rather than through a single response.

Linear interpolation of the existing release data placed the estimated 50% release time at approximately 4.5 h. Release increased by 34.3 percentage points during the first 4 h and by a further 44.4 percentage points from 4 to 24 h. The small difference between the first-order and Higuchi coefficients of determination was 0.008, confirming that both concentration-dependent and diffusion-associated descriptions were plausible, whereas the zero-order model provided substantially weaker agreement. These calculations are descriptive and do not replace independent kinetic experiments.

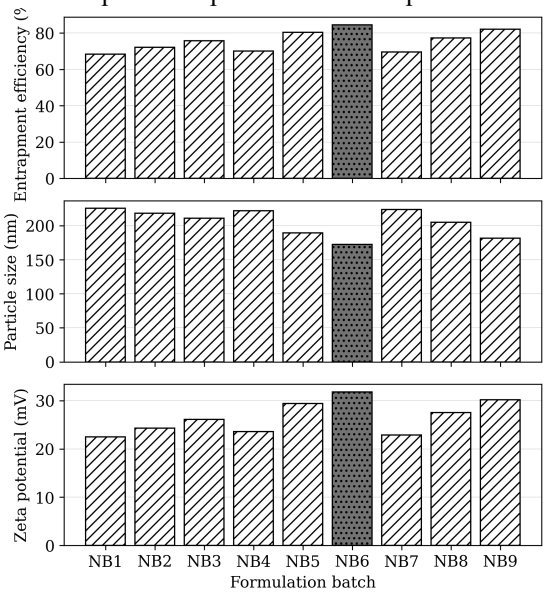

Figure 2. Comparative critical quality attributes of batches NB1-NB9; NB6 is identified by the solid gray bar.

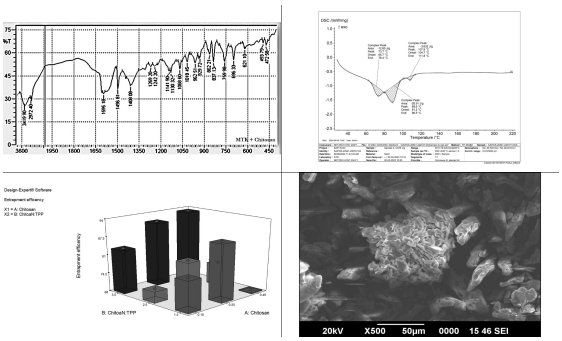

Figure 3. Original thesis characterization images: FTIR spectrum, DSC thermogram, entrapment-efficiency response graph, and SEM micrograph of the nanobiocomposite.

4. Discussion

Increasing chitosan does not produce a uniformly beneficial effect. More polymer can provide additional binding sites and raise drug retention, but it also increases solution viscosity and can enlarge particles if mixing and cross-linking become inefficient. TPP ratio likewise controls network density: insufficient cross-linker yields a loose matrix, whereas excessive cross-linker may produce local over-cross-linking or aggregation. The response pattern therefore supports optimization of the factor combination rather than maximization of either factor alone.

The positive zeta potential arises from residual protonated amino groups on chitosan. Values around +30 mV are commonly interpreted as supportive of electrostatic repulsion, although zeta potential cannot by itself prove long-term physical stability. The modest particle diameter of NB6 may assist reproducible dispersion and creates a large surface area, but aerodynamic behavior must be measured before claims about respirability or regional lung deposition can be made.

The two-phase release profile is mechanistically plausible for an ionically cross-linked matrix. Loosely associated surface drug can partition rapidly into the medium, while entrapped molecules encounter a longer diffusional pathway. The strong first-order fit indicates concentration dependence, and the Higuchi fit shows that square-root-of-time diffusion also describes much of the profile. Model fitting should be interpreted descriptively because several equations can fit a limited set of time points.

Microwave assistance offers process efficiency, yet it introduces additional variables including vessel geometry, load volume, field distribution and cooling rate. These factors can alter local temperature even when nominal power is unchanged. A scale-up strategy should therefore specify energy delivered per unit mass, real-time temperature monitoring and maximum exposure rather than relying only on appliance power.

Compatibility findings are reassuring but not definitive proof of chemical stability. FTIR band retention mainly excludes large structural changes, and DSC peak modification can reflect dilution, amorphization or polymer interaction. A stability-indicating chromatographic assay and impurity profile are required to distinguish benign physical transitions from low-level degradation.

The study's principal strength is the coherent use of factorial experimentation, multiple critical quality attributes and a functional release test. Its limitations include a small design space, indirect entrapment measurement, absence of a mass-balance report, and no aerosol or long-term stability data in the formulation-focused analysis. These limitations define the next experiments rather than negating the observed optimization signal.

4.1 Formulation Development Implications

Raw-material controls should begin with montelukast identity, assay, water content, solid form and particle characteristics. Chitosan should be specified by molecular-weight range, degree of deacetylation, viscosity in a stated solvent, residual protein, ash and microbial quality. TPP grade and ionic composition matter because cross-linking depends on available phosphate species. Supplier changes should trigger comparability testing rather than administrative substitution.

Solution preparation is a critical unit operation. Acetic-acid concentration determines protonation and solubility of chitosan, while mixing time determines whether polymer chains are uniformly hydrated. Entrained air can complicate volume measurements and later particle-size analysis. A manufacturing instruction should define order of addition, impeller type, vessel geometry, temperature, mixing speed and an objective endpoint for complete dissolution.

Drug addition requires a reproducible dispersion strategy. Montelukast that enters the polymer solution as uncontrolled crystals may be counted as encapsulated after centrifugation even if it is merely sedimented. Visual inspection should be supplemented by microscopy or filtration controls, and free-drug separation should be challenged to show that nanoparticles and crystals are not misclassified.

TPP addition controls the rate at which ionic junctions form. Slow addition can favor distributed nucleation, whereas a concentrated local bolus can create dense aggregates. Pump calibration, needle or nozzle geometry, addition position and agitation pattern are consequently scale-sensitive parameters. Recording total addition time is insufficient if the local mixing environment changes between batches.

Microwave exposure should be reported as a process rather than a single power setting. The temperature-time history, sample mass, vessel material, fill depth and cooling interval influence the actual energy experienced by the formulation. Drug assay before and

after processing, together with chromatographic impurity monitoring, is necessary to demonstrate that apparent process efficiency does not conceal degradation.

Centrifugation and washing affect both composition and recovery. Excessive force may compact particles irreversibly, whereas inadequate separation can leave free drug and TPP in the product. The mass of solids recovered, drug in each wash, and redispersibility after each cycle provide a clearer process balance. Losses to tubes and membranes should be examined during method qualification.

Lyophilization should use a protectant selected through redispersion studies. Freezing concentrates salts and can change local pH, while ice-crystal growth can exclude nanoparticles into narrow channels. Primary drying must remain below the relevant collapse temperature, and secondary drying must reduce moisture without promoting chemical change. Pre- and post-drying size, PDI, assay and release are useful comparability measures.

The UV assay is convenient for development, but specificity can be compromised by polymer, degradation products or turbidity. Blank nanobiocomposite, free-drug standards and spiked recovery samples should be evaluated. A chromatographic method is preferable for final assay and stability because it can separate montelukast from related substances and formulation components.

Dynamic light scattering requires standardized sample preparation. Dilution can change ionic strength and disrupt weak aggregates; sonication can artificially narrow the distribution or damage the carrier. The diluent, dilution factor, equilibration time, count rate, viscosity and refractive-index assumptions should be controlled. Replicate preparations are more informative than repeated readings from one cuvette.

An optimization model should report its equation, coefficient uncertainty, residual diagnostics, lack-of-fit assessment and predicted response at the selected condition. Confirmation batches prepared independently are essential because the numerically best design point may benefit from random experimental variation. Robustness is demonstrated when small deliberate changes remain within the acceptance region.

Release-method development should test membrane compatibility, receptor-medium solubility, agitation sensitivity and sampling replacement. Recovery at the final time should approach the known dose. A method that releases every batch too rapidly cannot discriminate formulation changes; a method that suppresses release through non-sink conditions is equally misleading.

Short-term dispersion stability can be assessed through size, PDI, surface potential, pH and visible sedimentation at controlled intervals. For dried material, moisture uptake, reconstitution time and post-reconstitution attributes become central. Chemical stability needs assay and degradants, not only unchanged appearance or particle size.

Scale-up should preserve dimensionless or mechanistically relevant quantities such as mixing time relative to addition time, energy input per volume and heat-removal capacity. Simply multiplying ingredient quantities while using the same stirring speed changes the hydrodynamic environment. Engineering batches should map these relationships before pivotal material is produced.

A route-specific performance test is the final bridge between nanoparticle metrics and use. For inhalation, emitted dose and aerodynamic size distribution are required. For oral administration, dissolution, gastrointestinal stability and absorption are relevant. The optimized NB6 profile is a development starting point, not a finished product specification.

5. Conclusion

Microwave-assisted ionic gelation produced montelukast sodium-loaded chitosan nanobiocomposites with formulation-dependent size, surface charge and entrapment. NB6 was the most balanced batch, achieving 84.6 ± 1.7% entrapment, 172.6 ± 4.2 nm particle size and +31.8 ± 1.1 mV zeta potential. Its sustained 24-h release and diffusion-associated kinetic behavior justify further development. Confirmation should include validated assay and impurities, aerosol performance, storage stability, scale-up robustness and pharmacokinetic comparison.

REFERENCES

1. Bhumkar, D. R., & Pokharkar, V. B. (2006). Studies on the effect of pH on cross-linking of chitosan with sodium tripolyphosphate. AAPS PharmSciTech, 7(2), Article 50.
2. Fu, Y., & Kao, W. J. (2010). Drug release kinetics and transport mechanisms of polymeric delivery systems. Expert Opinion on Drug Delivery, 7(4), 429-444.
3. Illum, L. (1998). Chitosan and its use as a pharmaceutical excipient. Pharmaceutical Research, 15, 1326-1331.
4. Lehr, C. M., Bouwstra, J. A., Schacht, E. H., & Junginger, H. E. (1992). In vitro evaluation of mucoadhesive properties of chitosan and other natural polymers. International Journal of Pharmaceutics, 78, 43-48.
5. Panyam, J., & Labhasetwar, V. (2003). Biodegradable nanoparticles for drug and gene delivery to cells and tissue. Advanced Drug Delivery Reviews, 55, 329-347.
6. Van der Lubben, I. M., Verhoef, J. C., Borchard, G., & Junginger, H. E. (2001). Chitosan and its derivatives in mucosal drug and vaccine delivery. Advanced Drug Delivery Reviews, 52, 139-144.
7. Desai, M. P., Labhasetwar, V., Walter, E., Levy, R. J., & Amidon, G. L. (1997). Size-dependent uptake of biodegradable microparticles in Caco-2 cells. Pharmaceutical Research, 14, 1568-1573.

8. Gao, L., Zhang, D., & Chen, M. (2008). Drug nanocrystals for poorly soluble drugs and their application as delivery systems. Journal of Nanoparticle Research, 10, 845-862.
9. Chithrani, B. D., Ghazani, A. A., & Chan, W. C. W. (2006). Size and shape dependence of nanoparticle uptake into mammalian cells. Nano Letters, 6(4), 662-668.
10. Chen, M., Liu, Y., Yang, W., Li, X., Liu, L., & Zhou, Z. (2011). Self-assembled nanoparticles of cholesterol-modified chitosan for drug delivery. Carbohydrate Polymers, 84, 1244-1251.
11. Kawashima, Y., Handa, T., Takenaka, H., Lin, S. Y., & Ando, Y. (1985). Controlled-release granules coated with a sodium polyphosphate-chitosan complex. Journal of Pharmaceutical Sciences, 74, 264-268.
12. Ma, Z., Yeoh, H. H., & Lim, L. Y. (2002). Formulation pH modulates drug interaction with chitosan nanoparticles. Journal of Pharmaceutical Sciences, 91, 1396-1404.
13. Bonsnes RW, Taussky HH. Colorimetric determination of creatinine by Jaffe reaction. J Biol Chem. 1945;158:581.
14. Borchert H, Shevchenko EV, Robert A, Mekis I, Kornowski A, Grübel G, Weller H. Determination of nanocrystal sizes: comparison of TEM, SAXS and XRD studies of monodisperse CoPt3 particles. Langmuir. 2005;21(5):1931-1936.
15. Borghi L, Schianchi T, Meschi T. Comparison of two diets for prevention of recurrent stones in idiopathic hypercalciuria. N Engl J Med. 2002;346(2):77-84.
16. Borsatti A. Calcium oxalate nephrolithiasis: defective oxalate transport. Kidney Int. 1991;39(6):1283-1288.
17. Bozkir AA, Saka OM. Chitosan nanoparticles for plasmid DNA delivery: effect of chitosan molecular structure on formulation and release characteristics. Drug Deliv. 2004;11:107-112.
18. Butterweck V, Khan S. Herbal medicine in the management of urolithiasis: alternative or complementary? Planta Med. 2009;75:1095-1103.
19. Caraway WT. Determination of uric acid in serum by carbonate method. Am J Clin Pathol. 1955;25:840-845.
20. Chaitanya AKD, Kumar MS, Reddy AM, Mukherjee NSV, Sumath MH, Ramesh A. Antiurolithiatic activity of Macrotyloma uniflorum seed extract on ethylene glycol induced urolithiasis in albino rats. J Innov Trends Pharm Sci. 2010;1:216-226.
21. Chandoke PS. When is medical prophylaxis cost-effective for recurrent calcium stones? J Urol. 2002;168:937-940.
22. Chandy T, Sharma CP. Chitosan beads and granules for oral sustained delivery of nifedipine: in vitro studies. Biomaterials. 1992;13:949-952.
23. Chaudhary A, Tandon C, Singla SK. Calcium oxalate crystal growth inhibition by aqueous extract of Tamarindus indica. Indian J Urol. 2009;24:105-111.
24. Chauhan BS. Ecology of two troublesome Asteraceae species of rainfed rice: Siam weed (Chromolaena odorata) and coat buttons (Tridax procumbens). Weed Sci. 2008;56:567-573.
25. Chen M, Liu Y, Yang W, Li X, Liu L, Zhou Z. Preparation and characterization of self-assembled nanoparticles of 6-O-cholesterol-modified chitosan for drug delivery. Carbohydr Polym. 2011;84:1244-1251.
26. Chenite C, Chaput C, Combes F, Jalal A. Temperature-controlled pH-dependent formation of ionic polysaccharide gels. WO Patent 99/07416; 1999.
27. Chithrani BD, Ghazani A, Chan WCW. Determining the size and shape dependence of gold nanoparticle uptake into mammalian cells. Nano Lett. 2006;6(4):662-668.
28. Chitra P, Ujjwala KA, Manjusha B, Sowmya M, Mrudula P, Yashwant D. Antibacterial activity of Tridax procumbens with special reference to nosocomial pathogens. Br J Pharm Res. 2011;1(4):164-173.
29. Christina AJM, Packia Lakshmi M, Nagarajan M, Kurian S. Modulatory effect of Cyclea peltata Lam. on stone formation induced by ethylene glycol treatment in rats. Clin Exp Pharmacol Physiol. 2002;24(2):77-79.
30. Chu CC, Zhong C. Organo-soluble chitosan salts and chitosan-derived biomaterials prepared thereof. US Patent US2011/0150999 A1; 2011.
31. Chunekar KC, Pandey GS. Bhavaprakasha Nighantu of Bhavamishra. Varanasi: Chaukhambha Bharathi Academy; 2010. p. 103-104.
32. Clark EP, Collip JB. A study of the Tisdall method for determination of blood serum calcium with suggested modification. J Biol Chem. 1925;63:461.
33. Deepa T, Vijayalakshmi R. Studies on phytochemical constituents and hairy root induction from leaf segments of Aerva lanata through Agrobacterium rhizogenes. Int J Curr Sci. 2012:11-13.
34. Deepak G, Sam S, Khan KH. Biochemical composition and antibacterial activities of Lantana camara plants with different flower colors. EurAsian J BioSci. 2009;3:69-77.
35. Desai MP, Labhasetwar V, Walter E, Levy RJ, Amidon GL. Mechanism of uptake of biodegradable microparticles in Caco-2 cells is size dependent. Pharm Res. 1997;14:1568-1573.

36. Deshmukh TA, Yadav BV, Badole SL, Bodhankar SL, Dhaneshwar SR. Antihyperglycaemic activity of alcoholic extract of Aerva lanata leaves in alloxan-induced diabetic mice. J Appl Biomed. 2008;6:81-87.
37. Dibua UE, Odo GE, Udengwu S, Esimone C. Cytotoxicity and antitubercular activity of Allium sativum and Lantana camara against mycobacterial isolates from people living with HIV/AIDS. Internet J Infect Dis. 2010;8(1).
38. Disney MD, Zheng J, Swager TM, Seeberger PH. Detection of bacteria with carbohydrate-functionalized fluorescent polymer. J Am Chem Soc. 2004;126(41):13343-13346.
39. Diwan PV, Tillo LD, Kulkarni DR. Steroid-depressed wound healing and Tridax procumbens. Indian J Physiol Pharmacol. 1983;27(1):32-36.
40. Eck SL, Alavi JB, Alavi A, Davis A, Hackney D, Judy K, Mollman J, Phillips PC, Wheeldon EB, Wilson JM. Treatment of advanced CNS malignancies with recombinant adenovirus H5.010RSVTK: a phase I trial. Hum Gene Ther. 1996;7(12):1465-1482.
41. Gnessin E, Lingeman JE, Evan AP. Pathogenesis of renal calculi. Turk J Urol. 2010;36(2):190-199.
42. Evan AP, Coe FL, Lingeman JE, Worcester E. Insights on the pathology of kidney stone formation. Urol Res. 2005;33:383-389.
43. Fernandez-Urrusuno R, Calvo P, Remunan-Lopez C, Vila-Jato JL, Alonso MJ. Enhancement of nasal absorption of insulin using chitosan nanoparticles. Pharm Res. 1999;16:1576-1581.
44. Fisher RS, Ho J. Potential new methods for antiepileptic drug delivery. CNS Drugs. 2002;16(9):579-593.
45. Fiske CH, Subbarow Y. Colorimetric determination of phosphate. J Biol Chem. 1925;56:375-381.
46. Freeman RE, Wicks B, Parmar B. Stakeholder theory and the corporate objective revisited. Organ Sci. 2004;15(3):364-369.
47. Gao L, Zhang D, Chen M. Drug nanocrystals for formulation of poorly soluble drugs and their application as potential drug delivery systems. J Nanopart Res. 2008;10(5):845-862.
48. Gaur RD, Sharma J, Painuli RM. Plants used in traditional healthcare of livestock by Gujjar community of Sub-Himalayan tracts, Uttarakhand, India. Indian J Nat Prod Resour. 2010;1:243-248.
49. Geng Y, Dalhaimer P, Cai S, Tsai R, Tewari M, Minko T, Discher DE. Shape effects of filaments versus spherical particles in flow and drug delivery. Nat Nanotechnol. 2007;2(4):249-255.
50. Ghisalberti EL. Lantana camara (Verbenaceae): a review. Fitoterapia. 2000;71:467-486.
51. Goldfarb DS, Fischer ME, Keich Y. Twin study of genetic and dietary influences on nephrolithiasis: report from Vietnam Era Twin Registry. Kidney Int. 2005;67(3):1053-1061.
52. Habila JD, Bello IA, Dzikwi AA, Musa H, Abubakar N. Total phenolics and antioxidant activity of Tridax procumbens Linn. Afr J Pharm Pharmacol. 2010;4(3):123-126.
53. Hagan SA, Coombes AG, Garnett MC, Dunn SE, Davies MC, Illum L, Davis SS. Polylactide-poly(ethylene glycol) copolymers as drug delivery systems: characterization of micelle-forming systems. Langmuir. 1996;12:2153-2161.
54. Haixiong G, Yong H, Jiang X, Cheng D, Yuan Y, Bi H, Yang C. Preparation, characterization and drug release behaviour of nimodipine-loaded amphiphilic triblock copolymer micelles. J Pharm Sci. 2002;91(6):1463-1473.
55. Havagiray R, Shashi A, Jain SK, Sabharwal M. Herbal treatment for urinary stones. Int J Pharm Sci Res. 2010;1:24-29.
56. He C, Kim SW, Lee DS. In situ gelling stimuli-sensitive block copolymer hydrogels for drug delivery. J Control Release. 2008;127(3):189-207.
57. Illum L. Chitosan and its use as a pharmaceutical excipient. Pharm Res. 1998;15:1326-1331.
58. Irvine FR. Woody plants of Ghana. London: Oxford University Press; 1961.
59. Jadhav AD, Sawant MTB, Chavadar S. Extraction and antibacterial evaluation of extracts of Tridax procumbens. J Pure Appl Microbiol. 2011;5(1):343-347.
60. Jaeger P, Robertson WG. Role of dietary intake and intestinal absorption of oxalate in calcium stone formation. Nephron Physiol. 2004;98(2):64-71.
61. Jain H. Formulation and evaluation of analgesic activity of Tridax procumbens gel. Indian J Nat Prod. 2006;23(1):31-33.
62. Jasmine R, Selvakumar BN, Daisy P. Saponins from Eugenia jambolana with antimicrobial activity. Clin Microbiol Rev. 2007;12:564-582.
63. Kadiyala I, Loo Y, Roy K, Rice J, Leong KW. Transport of chitosan–DNA nanoparticles in human intestinal M-cell model versus normal intestinal enterocytes. Eur J Pharm Sci. 2010;39:103-109.
64. Kannaiyan S. An overview on Biological Diversity Act-2002. Int Biodiversity Day Souvenir. 2007:1-11.
65. Kawashima Y, Handa YT, Takenaka H, Lin SY, Ando Y. Novel method for preparation of controlled-release theophylline granules coated with sodium polyphosphate–chitosan complex. J Pharm Sci. 1985;74:264-268.

66. Khan SK, Rahman AHMM, Alam MS, Ahmed F, Islam AKM, Rafiul AKM, Rahman MM. Taxonomic studies on the family Asteraceae of Rajshahi Division. Res J Agric Biol Sci. 2008;4(2):134-140